

# The Rise and Fall of the Star Formation Histories of Blue Galaxies at Redshifts $0.2 < z < 1.4$

Camilla Pacifici, Susan Kassin, Ben Weiner, Stephane Charlot, Jonathan Gardner

ApJL 2013 - camilla.pacifici@galaxy.yonsei.ac.kr



## Introduction

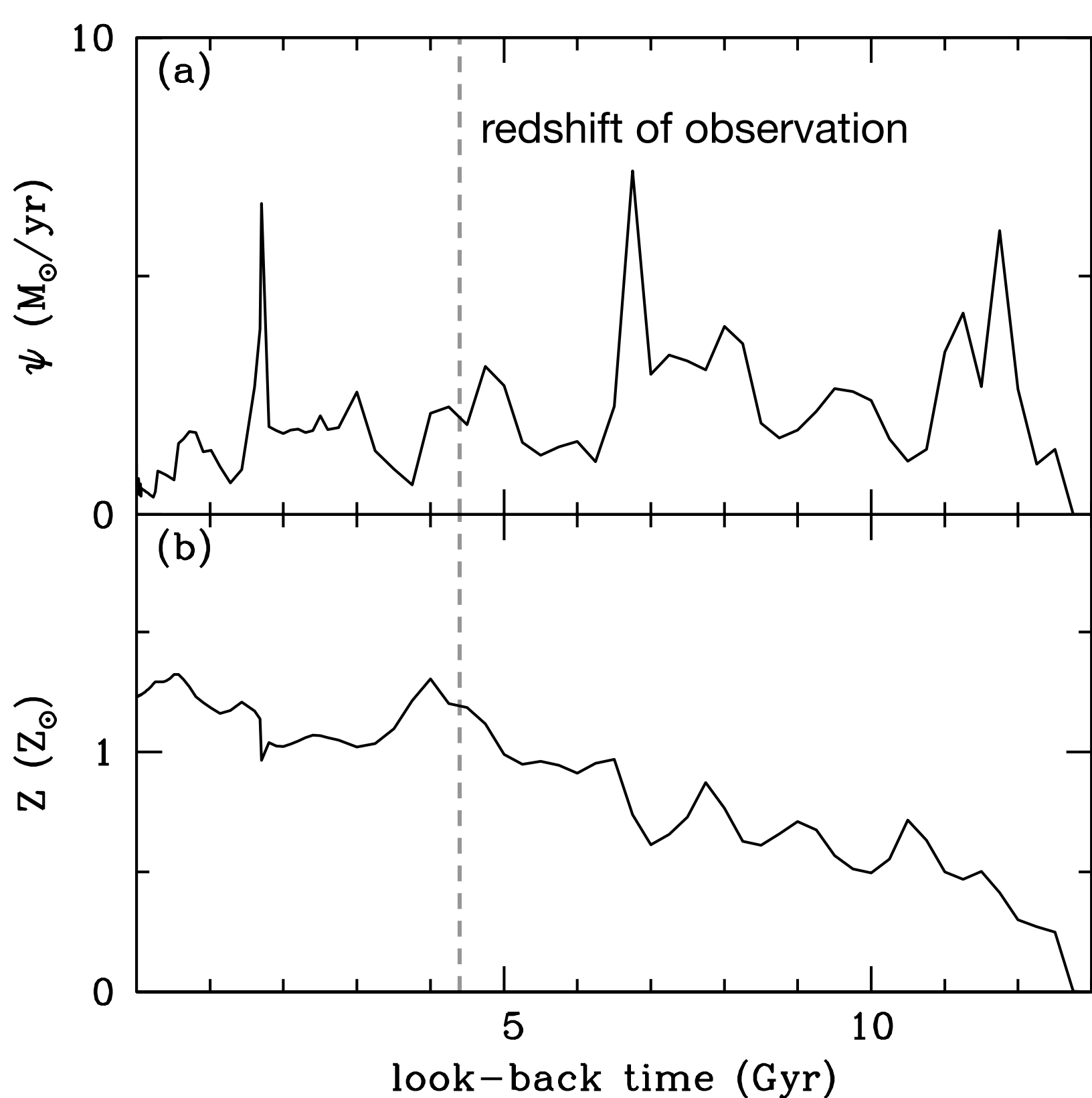
Constraints on the stellar content of galaxies are often derived from multi-wavelength observations by assuming that the star formation history (SFH) of an individual galaxy can be approximated by a simple declining exponential function of the form  $\exp(-t/\tau)$ , where  $t$  is the galaxy age and  $\tau$  the star formation timescale. Such “ $\tau$ -models” have been used successfully to estimate, for example, the stellar masses of nearby spiral galaxies from fits of rest-frame optical/near-infrared colors (e.g., Bell & de Jong 2001). Despite this success, an increasing number of analyses have pointed out the limitations of  $\tau$ -models, particularly for applications to studies of high-redshift galaxies. **To better characterize the SFHs of galaxies at moderate and high redshift, we require more sophisticated, physically motivated spectral analysis tools (Pacifici et al. 2012).**

## Data

From the AEGIS catalog, we extract 4517 potentially star-forming galaxies ( $U - B < 1.0$ ) with available photometry at  $B$ ,  $R$ ,  $I$  (Coil et al. 2004) and  $K_s$  (Bundy et al. 2006). For all galaxies, Keck/DEIMOS spectra are available from the DEEP2 Redshift Survey (Newman et al. 2012) with solid spectroscopic redshifts. We extract reliable fluxes of  $[\text{OII}]\lambda\lambda 3726.0, 3728.8$ ,  $\text{H}\beta$ ,  $[\text{OIII}]\lambda 5007$ , and  $\text{H}\alpha$  (Weiner et al. 2007), when these lines fall into the observed wavelength range of the spectra.

## Modeling approach

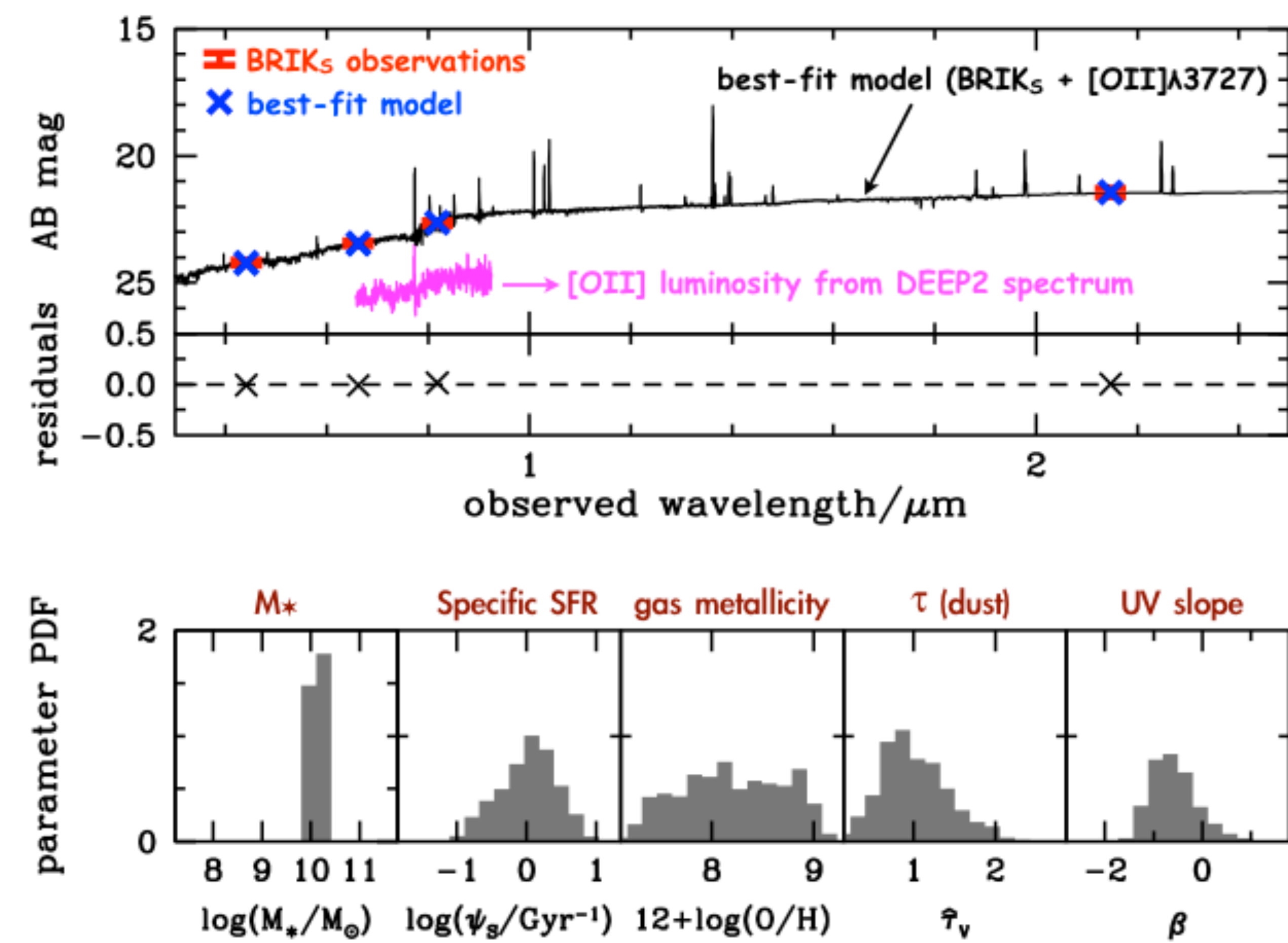
We build a comprehensive library of model star formation and chemical enrichment histories by performing a **post-treatment of the Millennium cosmological simulation** (Springel et al. 2005) using the semi-analytic models of De Lucia & Blaizot (2007). We generate a library of 1 million galaxy SEDs by combining this library of star formation and chemical enrichment histories with the latest version of the Bruzual & Charlot (2003) **stellar population synthesis models**, the galaxy **nebular emission model** of Charlot & Longhetti (2001) (based on the photoionization code CLOUDY; Ferland 1996), and the **2-component dust model** of Charlot & Fall (2000).



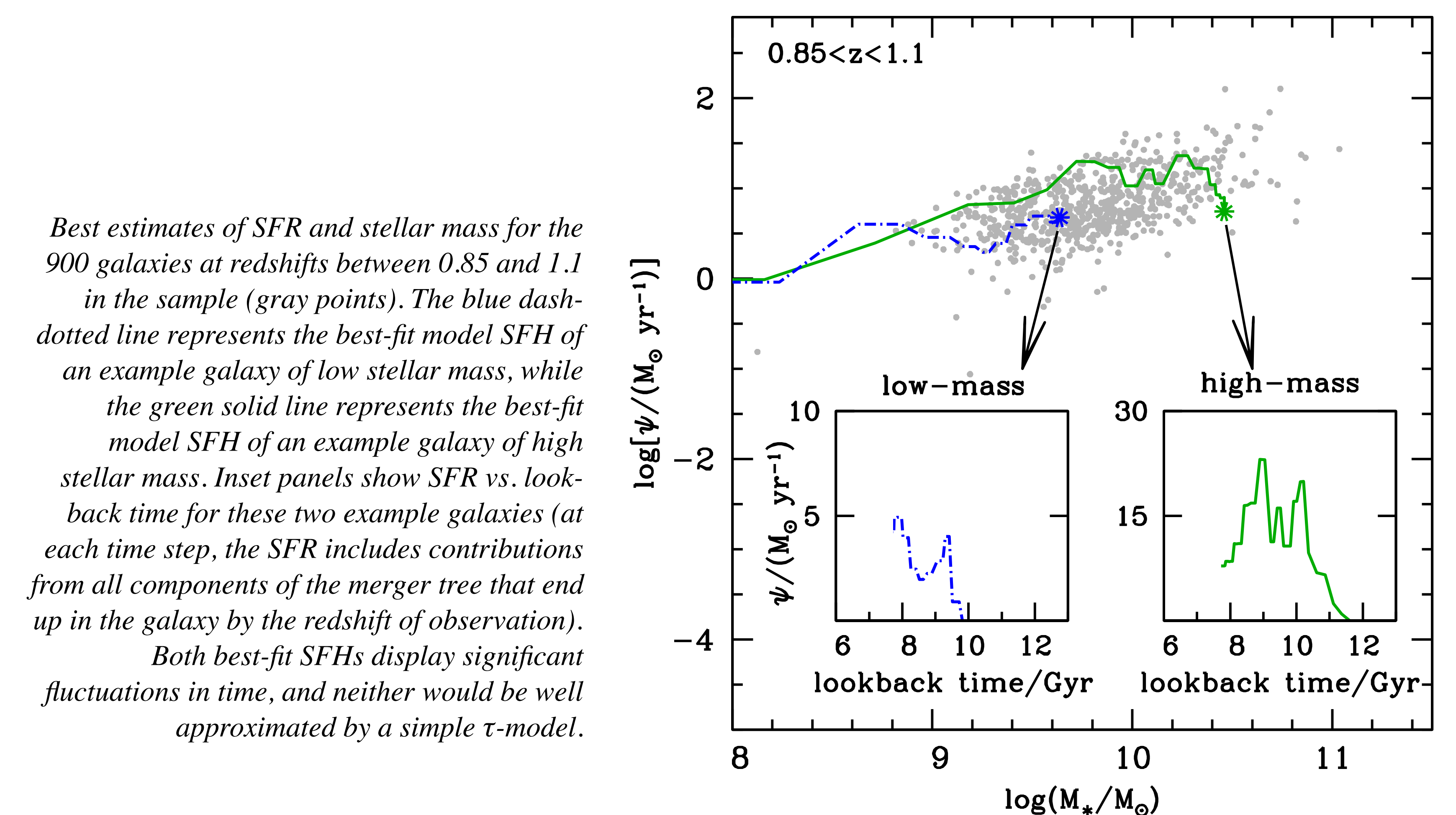
Example of galaxy star formation and chemical enrichment histories inferred from the semi-analytic post-treatment of the Millennium cosmological simulation: (a) star formation rate,  $\psi$ , and (b) interstellar metallicity,  $Z$ , plotted as a function of look-back time, for a galaxy with a present-day stellar mass of  $1.5 \times 10^{10} M_{\odot}$ .

## Fitting procedure

For each galaxy in the sample, we compute the likelihood that each model in the library reproduces the observed SED. Specifically, we compare the observed and modeled photometric fluxes in the  $B$ ,  $R$ ,  $I$  and  $K_s$  bands (observer frame) and the **emission-line luminosities of  $[\text{O II}]$ ,  $\text{H}\beta$ ,  $[\text{O III}]$  and/or  $\text{H}\alpha$** . For each observed galaxy, we use the computed model likelihoods to build the probability density functions of stellar mass,  $M_*$ , and SFR,  $\psi$  (normalized to the absolute observed  $K_s$ -band luminosity). For each galaxy in the sample, we also retain the best-fit SFH.



Spectral fit of one example galaxy. Top panel: BRICKs observed magnitudes (red dots), BRICKs magnitudes of the best-fit model galaxy (blue crosses), best-fit model spectrum (black line), DEEP2 observed spectrum (magenta line). Middle panel: residuals between best-fit model magnitudes and data (crosses). Bottom panels: probability density functions retrieved for stellar mass, specific star formation rate, gas-phase oxygen abundance, total effective optical depth of the dust, and rest-frame ultraviolet slope.

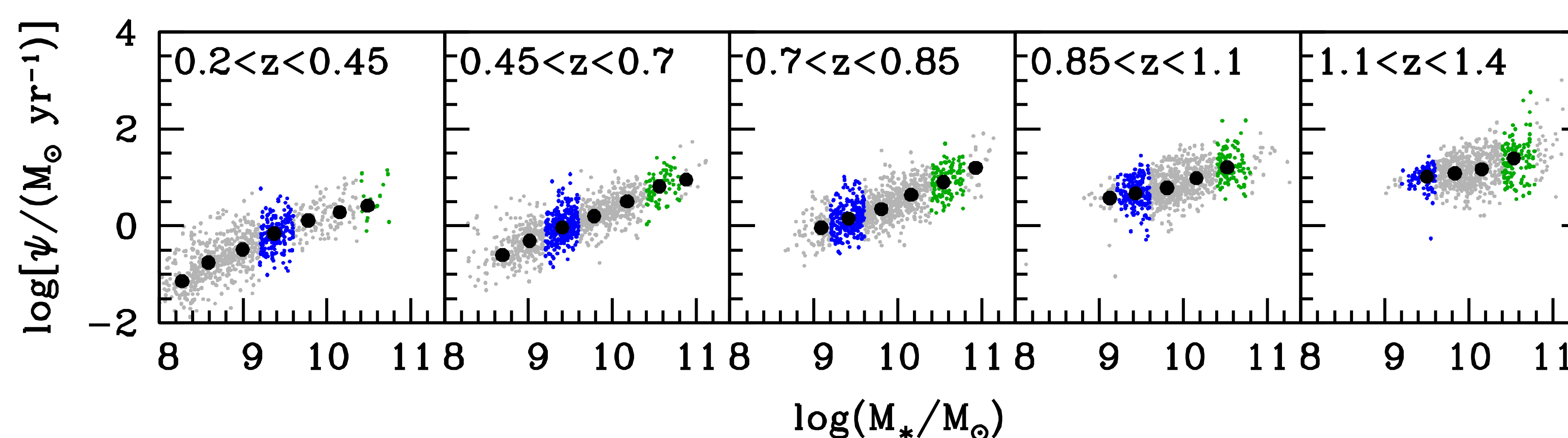


Best estimates of SFR and stellar mass for the 900 galaxies at redshifts between 0.85 and 1.1 in the sample (gray points). The blue dash-dotted line represents the best-fit model SFH of an example galaxy of low stellar mass, while the green solid line represents the best-fit model SFH of an example galaxy of high stellar mass. Inset panels show SFR vs. look-back time for these two example galaxies (at each time step, the SFR includes contributions from all components of the merger tree that end up in the galaxy by the redshift of observation). Both best-fit SFHs display significant fluctuations in time, and neither would be well approximated by a simple  $\tau$ -model.

## Conclusions

The best-fit SFHs of individual galaxies exhibit characteristic fluctuations arising from the merger histories, which cannot be well described by simple  $\tau$ -models. At all redshifts ( $0.2 < z < 1.4$ ), the average SFH of **high-mass blue galaxies** ( $\sim 4 \times 10^{10} M_{\odot}$ ) **rises and falls in a bell-shaped manner**, suggesting that these galaxies are gradually turning off their star formation activity. **The average SFH of low-mass galaxies** ( $\sim 3 \times 10^9 M_{\odot}$ ) **keeps rising in a more extended way**. The shapes of the SFHs suggest that, at any redshift, **low-mass galaxies have on average higher specific SFR** ( $\psi_s = \psi / M_*$ ) **than high-mass galaxies**, consistent with the trends in the star formation main sequence (e.g., Noeske et al. 2007) and in the latest simulations of Behroozi et al. (2012). At fixed stellar mass, **the shape of the average SFH is independent of galaxy redshift**, although the evolution proceeds faster in the most distant galaxies. At fixed redshift, the look-back time by which half the stellar mass of a galaxy has formed (vertical dashed lines in the figures below) increases with stellar mass.

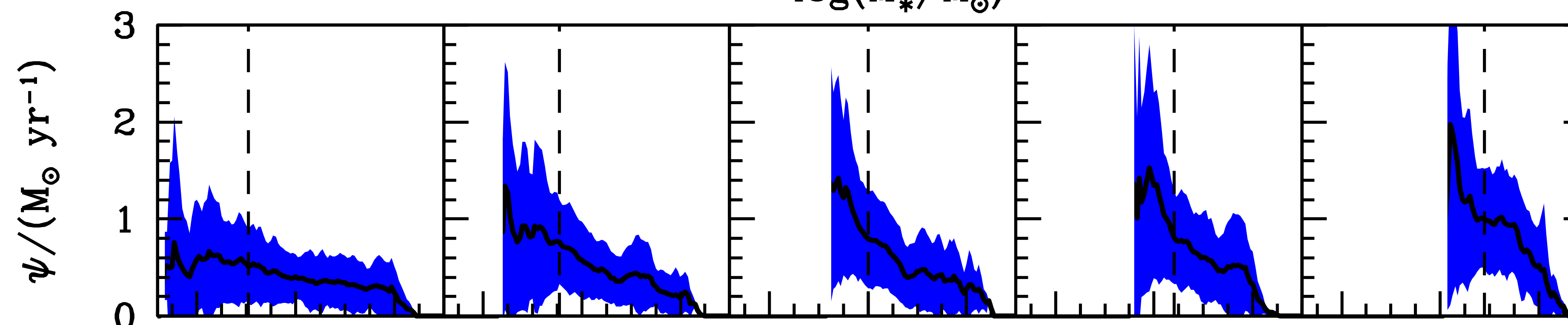
## Main sequence



Star formation main sequence (i.e., SFR vs. stellar mass) for the galaxies in five redshift bins spanning the range  $0.2 < z < 1.4$ . A bin of low-mass galaxies ( $M_* = 1.6\text{--}4.0 \times 10^9 M_{\odot}$ ) is highlighted in blue, and one of high-mass galaxies ( $M_* = 2.5\text{--}6.3 \times 10^{10} M_{\odot}$ ) highlighted in green.

## Low-mass galaxies

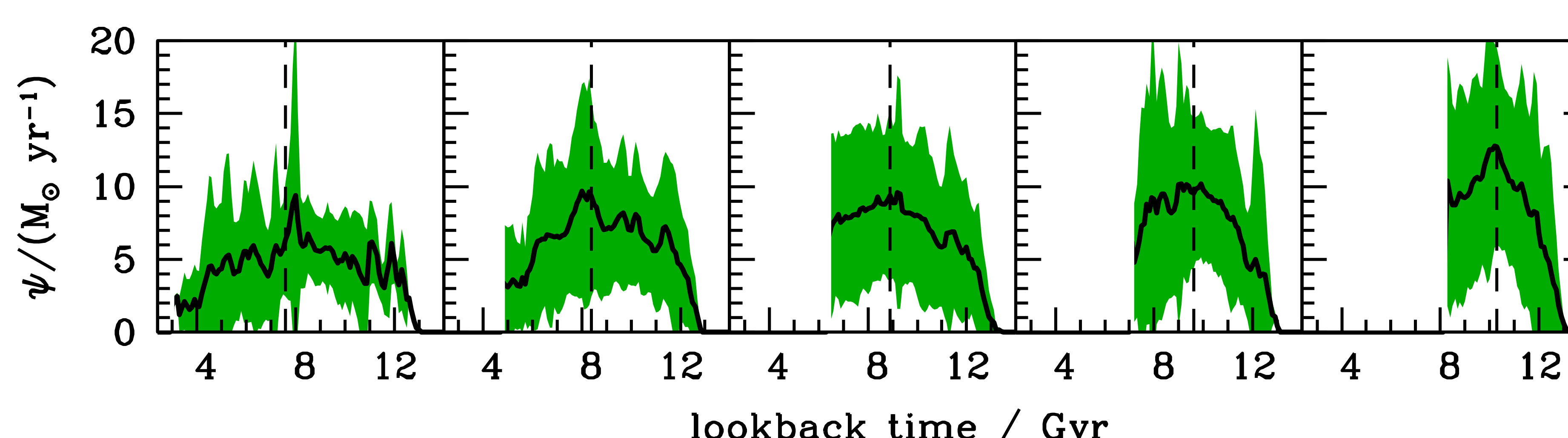
Rising in an extended way



Average best-fit SFHs of the galaxies in the low-mass bin, in the same redshift bins spanning the range  $0.2 < z < 1.4$  from left to right (black solid line), and root mean square deviations about these averages (blue shadow). At any redshift, the average SFH of low-mass galaxies keeps rising in an extended way, inconsistent with declining  $\tau$ -models.

## High-mass galaxies

Rise and fall, bell-shaped



Average best-fit SFHs of the galaxies in the high-mass bin, in the same redshift bins spanning the range  $0.2 < z < 1.4$  from left to right (black solid line), and root mean square deviations about these averages (green shadow). At any redshift, the average SFH of high-mass galaxies rises and falls in a bell-shaped manner, which cannot be approximated by simple exponentially declining or rising  $\tau$ -models.